Electronic Supplementary Material (ESI) for ChemComm.

Pre-targeting of PEG nanomaterials to balance tumour accumulation and clearance

N. L. Fletcher,*[a] A. Prior,[a] O. Choy,[a] J. Humphries,[a] P. Huda,[a] S. Ghosh,[a] Z. Houston,[a] C. Bell[a] and K. J. Thurecht*[a]

[a]Centre for Advanced Imaging, Australian Institute for Bioengineering and Nanotechnology and ARC Training Centre for Innovation in Biomedical Imaging Technology, The University of Queensland, Brisbane, Australia;

1. Materials and methods

1.1. Materials

1.1.1. Reagents

Azobis(isobutyronitrile) (AIBN; Sigma Aldrich) was recrystallised twice from methanol before use. Tetrahydrofuran (THF) and n-Hexane were used dry where appropriate and of reagent grade. Poly(ethylene glycol) methyl ether methacrylate (PEGMA, Mn = 500 g mol-1) (Sigma Aldrich 98%) and ethylene glycol dimethacrylate (EGDMA, Sigma Aldrich 98%) were removed from inhibitor prior to use by passing through an activated basic alumina plug (Al_2O_3: Sigma Aldrich, Brockmann I, standard grade, ~150 mesh, 58 Å). Triethylamine (TEA, Sigma-Aldrich, ≥99%), 2-Mercaptothiazoline (≥98% Sigma Aldrich) 1-ethyl-3-(3-(dimethylamino)propyl) carbodiimide hydrochloride (EDC, Fluorochem, 99%), Deferoxamine-dibenzocyclooctyne (DFO-DBCO; Product B-773, MW 848) and Deferoxamine-isothiocyanate (DFO–Bz–NCS; Product B-705, MW 752.9) (Macrocyclics), Azido-PEG3-Amine (Click Chemistry Tools), Cyanine-5 amine (Cy5) (Lumiprobe) and Fluorescein isothiocyanate isomer I (Sigma; F7250) were used as received. 4-cyano-4-(ethylsulfanylthiocarbonyl)sulfanylpentanoic acid (CEPA) was synthesized according to a prior report.[1] BOC-amine CEPA was synthesised according to the method of Ediriweera *et al*.[2] BOC-amine ACVA was synthesised according to the method of Nadres *et al*.[3] Dimethyl sulfoxide-d6 (DMSO-d6) and deuterated chloroform (CDCl3) were purchased from Cambridge Isotope Laboratories, Inc.

Dulbecco's Modified Eagle Medium (DMEM; Gibco 10313021) and Penicillin-Streptomycin-Glutamine (PSG; 100X; Gibco 10378016) were obtained from ThermoFisher Scientific. Foetal Bovine Serum (FBS) was obtained from Moregate BioTech (Australia) and heat inactivated (56 °C for 1 hour) before use.

^{89}Zr in 1 M oxalic acid was obtained from Perkin Elmer and used for radiolabelling of materials within 2 days of receipt.

1.1.2. Bispecific Antibody Production

Bispecific Antibodies (BsAbs) were produced in house for this study. BsAbs comprising two single chain variable regions (ScFvs), one specific for human epidermal growth factor receptor (EGFR), the other for methoxy polyethylene glycol (mPEG) linked by a glycine serine (G4S) linker were expressed in CHO cells and purified through a series of size exclusion and affinity

chromatography steps as previously reported.[4] Purified α-EGFR/α-PEG BsAbs ($BsAb_{\alpha\text{-EGFR}/\alpha\text{-PEG}}$) were aliquoted in PBS, stored at -80 °C and thawed immediately before use.

1.2. Characterization

1.2.1. Nuclear Magnetic Resonance (NMR)

All NMR experiments were conducted on a Bruker Avance 500 MHz high-resolution NMR spectrometer. Diffusion-weighted spectra (DOSY) were collected at a gradient strength (gpz6) of 50% for a minimum of 128 scans. Chemical shifts are reported as δ in parts per million (ppm) and referenced to the chemical shift of the residual solvent resonances (CDCl3 1H: δ = 7.26 ppm; DMSO-d6 1H: δ = 2.50 ppm). The resonance multiplicities are described as s (singlet), d (doublet), t (triplet), q (quartet), m (multiplet) or br (broad).

1.2.2. Analytical Size Exclusion Chromatography (SEC)

SEC analysis of $HBP_{Cy5/DFO}$ was performed on a SEC-multi-angle laser light scattering (MALLS) chromatographic system consisted of a 1515 isocratic pump (Waters), a 717 autosampler (Waters), Styragel HT 6 E and Styragel HT 3 columns (Waters), 2414 differential refractive index detector (Waters) and a Dawn Heleos laser light scattering detector (Wyatt). THF was used as the mobile phase throughout with a flow rate of 1 mL/min. Molar mass (Mn, SEC) and dispersity (Đ) values of samples were determined on Waters software.

SEC analysis of HBP_{Block} was performed using a Shimadzu modular system comprising a DGU-405 degasser, a SIL-40C XR auto sampler, and a LC-40D XR solvent delivery module. Wyatt technologies Optilab and miniDAWN detectors were used for collection of RI and MALS data. A shim-pack GPC-800DP 5.0 µm bead-size guard column (10 × 4.6 mm), followed by a shim-pack GPC-80MD column (300 × 8 mm) were maintained at 40°C with a CTO-40C oven. Dimethylformamide with 0.03% w/v LiBr at a flow rate of 1 mL min-1 was used as the eluent. Polystyrene standards were used for calibration. Analyte samples were filtered through 0.45 µm PTFE filters before injection. Molar mass (Mn, SEC) and dispersity (Đ) values of samples were determined on Shimadzu LabSolutions software.

1.2.3. Ultraviolet-Visible Spectroscopy (UV-Vis)

UV–Vis was performed on a Nanodrop 2000C spectrophotometer (Thermo Scientific) using a quartz-glass pedestal with 1 mm path length.

1.3. Antibody functionalization and Polymer Synthesis

1.3.1. BsAb dye labelling

For *in vitro* assays to monitor BsAb binding and internalization, $BsAb_{\alpha\text{-EGFR}/\alpha\text{-PEG}}$ was conjugated with fluorescein isothiocyanate (FITC). 50% v/v of 0.1 M Na_2CO_3, pH 9.2 was added to BsAb at 4.5 mg/mL in PBS to bring the pH to slightly alkaline. FITC was dissolved in DMSO at 10 mg/mL and added at 10-fold molar excess to the BsAb. The reaction was incubated at 4 °C overnight with mixing by inversion on an IKA Loopster basic system. To remove free dye from the sample, the reaction mixture was buffer exchanged into PBS through a 7 kDa cut-off Zeba Spin desalting column. Final $BsAb_{\alpha\text{-EGFR}/\alpha\text{-PEG}/FITC}$ protein concentration was determined by UV-Vis

analysis of protein absorption at 280 nm. Samples were stored at 4 °C until use in flow cytometry and microscopy studies.

1.3.2. BsAb chelator functionalization

For BsAb pharmacokinetic studies, $BsAb_{\alpha\text{-EGFR}/\alpha\text{-PEG}}$ was conjugated to isothiocyanate functionalized Deferoxamine (DFO–Bz–NCS) a bifunctional chelate, prior to radiolabelling with [^{89}Zr]. BsAb concentration was adjusted to approximately 2 mg/ml in PBS and buffer exchanged to 0.1 M Na_2CO_3, pH 9.0 using a 10 kD cut-off Amicon® Ultra 0.5 mL centrifugal filter (Merck Millipore). DFO–Bz–NCS was dissolved in DMSO at a concentration of 10 mM (7.6 mg/mL). 5-fold molar excess of this chelator was added to $BsAb_{\alpha\text{-EGFR}/\alpha\text{-PEG}}$ and reaction mixture incubated for 1 hour at 37 °C using a Thermomixer rotating at 550 rpm. To remove free chelate from the sample, reaction mixtures were buffer exchanged in PBS 8-10 times using 10 kD cut-off centrifugal filters. Final $BsAb_{\alpha\text{-EGFR}/\alpha\text{-PEG/DFO}}$ protein concentration was measured using a standard bicinchoninic acid (BCA) assay kit (Pierce™, Thermo) following manufacturer's instructions. Samples were stored at -20 °C in small aliquots and thawed immediately before radiolabelling with [^{89}Zr].

1.3.3. Chain Transfer Agent Synthesis

4-Cyano-4-(ethylsulfanylthiocarbonylsulfanyl)pentanoic acid (CEPA) (0.25 g, 0.95 mM), 2-Mercaptothiazoline (0.226 g, 1.9 mM), and 4-Dimethylaminopyridine (DMAP) (0.023 g, 0.19 mM) were dissolved in 5 mL ice-cold dry dichloromethane (DCM) in a two-necked round bottom flask. The reaction was purged with nitrogen for 5 minutes, then N-ethylcarbodiimide hydrochloride (EDC.HCl) (0.364 g, 1.9 mM) was added under nitrogen. The reaction flask was sealed and allowed to stir on ice for 6 hours, then filtered and concentrated under vacuum. The crude was purified by column chromatography (silica; EtOAc:n-Hexane = 1:3), yielding the purified product, CEPA-TT as a yellow solid (0.23 g, 92%).

^{1}H NMR (500 MHz, $CDCl_3$): 4.59 ppm (t, 2H, H_f), 3.64 – 3.51 ppm (m, 2H, H_g), 3.38 – 3.30 ppm (m, 4H, $H_{b,e}$), 2.64 – 2.46 ppm (m, 2H, H_d), 1.89 ppm (s, 3H, H_c), 1.36 ppm (t, 3H, H_a).

1.3.4. Hyperbranched Polymer Synthesis

1.3.4.1. HBP_{Core} synthesis

PEGMA (0.275 g, 0.55 mM), ethylene glycol dimethacrylate (0.0065 g, 0.033 mM), CEPA-TT (0.010 g, 0.027 mM), AIBN (0.0009 g, 0.0054 mM), and Cy5-MA (0.0015 g, 0.0023 mM) were dissolved in 0.49 mL of dry THF and transferred to a dry Young's Tapped Schlenk flask. The reaction mixture was degassed via freeze–pump–thaw five times, backfilled with Ar, and then polymerized for 48 h at 65 °C with stirring. The crude polymer was then precipitated into cold n-Hexane and allowed to settle overnight at −20 °C. The supernatant was discarded, and the process was repeated, after which the purified polymer, HBP_{Core} was dried under vacuum to yield a blue oil (0.209 g, 76%).

^{1}H NMR (500 MHz, DMSO-d_6): 4.04 ppm (s, 2H, H_b, PEGMA), 4.55 ppm (br, 2H, H_a, CEPA-TT). Diagnostic peaks from UV–vis: λ_{max} = 309 nm, ε = 16200 M^{-1} cm^{-1} (thiocarbonyl π-π* absorption band), λ_{max} = 647 nm, ε = 250000 M^{-1} cm^{-1} (Cy5).

1.3.4.2. HBP_{Core} DFO conjugation to form $HBP_{Cy5/DFO}$

HBP_{Core} (0.05 g, 0.005 mM) was dissolved in 100 uL DMSO. Deferoxamine-DBCO (0.013 g, 0.015 mM) was dissolved in 20 uL DMSO. Azido-PEG3-Amine (0.0013 g, 0.006 mM) was dissolved in 50 uL dimethyl sulfoxide (DMSO). 5 uL of triethylamine (TEA) was added and the solution was allowed to stir for 5 minutes at room temperature, before being added to the vial containing HBP_{Core}. The reaction was stirred at room temperature for 5 minutes, then the solution containing Deferoxamine-DBCO was added dropwise while stirring. The reaction proceeded overnight at room temperature, then was diluted in Milli-Q water and dialyzed overnight against Milli-Q water in 3.5 kDa molecular weight cutoff pleated snakeskin dialysis tubing. After dialysis, the polymer solution was collected and further purified with an AKTA Prime Plus (GE) utilizing dual HiTrap desalting columns (GE) in 4:1 H2O/EtOH mix. The first major peak was collected, and the ethanol was removed under vacuum, after which the polymer was lyophilized and the process repeated a further 3 times until only the first peak was observed to elute. The final polymer conjugate, $HBP_{Cy5/DFO}$, was dried under vacuum then lyophilized to yield a pale blue oil (0.032 g, 64%).

^{1}H NMR (500 MHz, DMSO-d_6): 4.04 ppm (s, 2H, H_b, PEGMA), 7.10 – 7.94 ppm (m, H_a, DFO-DBCO). Diagnostic peaks from UV–vis: λ_{max} = 309 nm, ε = 16200 M^{-1} cm^{-1} (thiocarbonyl π-π* absorption band), λ_{max} = 647 nm, ε = 250000 M^{-1} cm^{-1} (Cy5). $M_{n,NMR}$ = 11.4 kDa; $M_{n,SEC\text{-}MALLS}$ = 46 kDa; $Đ_M$ = 1.37.

The M_n of each polymer chain in the HBP was determined from integration of the RAFT end group (a) with respect to the PEGMA monomer peak (b; Figure S3) to give the degree of polymerization. The number of chains per HBP can then be determined by comparison of the chain Mn to the total HBP Molar Mass as determined by SEC-MALLS as we have previously reported.[5] The resulting values are presented in Table 1.

1.3.4.3. HBP_{Block} Synthesis

A non-dye or chelator functionalized PEG based HBP was synthesized in a similar method to those above to yield an equivalent material for use as a blocking agent in binding assays.

PEGMA (2.0 g, 5.01 mmol), EGDMA (0.0436 g, 0.272 mmol), BOC-amine CEPA (81.3 mg, 0.263 mmol) and BOC-amine ACVA (22.7 mg, 0.052 mmol) were dissolved in 1,4-dioxane (4 mL) then transferred to a Young's tapped ampoule. The solution was then degassed by freeze-pump-thaw (3 cycles), backfilled with argon, sealed, and submerged in an oil bath at 65 °C for 48 h. The resultant solution was then dialysed against Milli-Q water for 3 days in 3.5 kDa molecular weight cut-off pleated snakeskin dialysis tubing with vigilant changing of water and then lyophilised. The polymer residue was then dissolved in THF and precipitated into cold diethyl ether and left to settle at -20 °C overnight. The supernatant was decanted, the oily residue dissolved in CH_2Cl_2, and the purification process repeated. The final product was dried under high vacuum at 25 °C overnight to yield a highly viscous yellow oil (1.8 g, 84%).

^{1}H NMR (500 MHz, DMSO-d_6): 4.04 ppm (s, 2H, H_b, PEGMA), 1.44 ppm (s, 9H, H_a, BOC-amine CEPA), $M_{n,NMR}$ = 11.0 kDa. Diagnostic peaks from UV–Vis: λ_{max} = 309 nm, ε = 16200 M^{-1} cm^{-1} (thiocarbonyl π-π* absorption band). SEC-MALLS (DMF): $M_{n,SEC\text{-}MALLS}$ = 17.9 kDa; $Đ_M$ = 1.38.

1.4. *In vitro* assay methods

1.4.1. Cell culture

Human breast cancer MDA-MB-468 cells (ATCC; $EGFR^+$) were maintained in DMEM containing 10% (v/v) FBS and 1XPSG at 37 °C in 5% CO_2. Cells were harvested from tissue culture flasks using Trypsin (0.15%), centrifuged at 200 g for 5 minutes before being resuspended in complete media and seeded as required for flow cytometry, confocal microscopy or tumour inoculation below.

1.4.2. Flow Cytometry

50,000 MDA-MB-468 cells were seeded in wells of a 24-well plate in 1 mL complete media and incubated for 48 hours at 37°C with 5% CO_2 to allow cells to adhere. Media was removed and treatments ($HBP_{Cy5/DFO}$, $BsAb_{\alpha\text{-EGFR}/\alpha\text{-PEG}}$, $BsAb_{\alpha\text{-EGFR}/\alpha\text{-PEG/FITC}}$ or $HBP_{Cy5/DFO}$+$BsAb_{\alpha\text{-EGFR}/\alpha\text{-PEG}}$ $_{+/\text{-FITC}}$ at varied ratios) were added to individual dishes in 250 µL volumes and incubated for the required times at 37°C with 5% CO_2. For all HBP incubated samples, 5 µg $HBP_{Cy5/DFO}$ was added per well.

For all in vitro and in vivo Premix samples, HBP was incubated with BsAb for 45 minutes at room temperature prior to addition to cells or injection into animals. Given the previously reported studies of antigen binding for this BsAb,[6] we expect association of BsAb with HBP to be complete within much shorter timeframes, however this has not been specifically optimized. This length of time is regularly utilized in antibody staining protocols and is maintained at this relatively long time for consistency with our previous studies.[6-9] We do not anticipate or observe this causing issues with aggregation but ensures complete equilibration of association prior to interactions with cells and tumours.

$BsAb_{\alpha\text{-EGFR}/\alpha\text{-PEG}}$ and HBP_{Block} amounts were calculated based on specified stoichiometry to $HBP_{Cy5/DFO}$ at the specified timings. For pre-targeting samples, dishes were rinsed 3-fold with 1 mL PBS after removing BsAb containing media before adding either complete media, or complete media containing HBP as specified.

After the specified incubation times at 37°C with 5% CO_2, treatments were then removed and cells were washed twice with 1 mL PBS before being detached using 0.5 mL enzyme-free dissociation buffer. Cells were then collected and wells rinsed with a further 0.5 mL PBS before centrifugation at 200 x g for 5 minutes (RT). Supernatants were removed and the cell pellets resuspended in 200 µL PBS and kept on ice until flow cytometry analysis.

Samples were analysed on a CytoFLEX (BRV series, Beckman Coulter) using 60 µL/min flow rate and 10,000 cell events (as determined from forward-side scatter gating) collected per sample. Fluorescence of each event was recorded with Cy5 detected using 638 nm laser excitation and 660/20 BP or 780/60 BP (to avoid any contribution from FITC in FITC containing samples) emission and FITC detected using 488 nm laser excitation and 525/40 BP emission. Data analysed using CytExpert (Beckman Coulter) and plotted as % positive relative to cell alone samples and measured median fluorescent intensity of events in appropriate channels.

1.4.3. Confocal Microscopy

50,000 MDA-MB-468 cells were seeded in 33mm µ-Dishes in 1 mL complete media and incubated for 48 hours at 37°C with 5% CO_2 to allow cells to adhere. Media was removed and treatments ($HBP_{Cy5/DFO}$, $BsAb_{\alpha\text{-EGFR}/\alpha\text{-PEG}}$, $BsAb_{\alpha\text{-EGFR}/\alpha\text{-PEG/FITC}}$ or $HBP_{Cy5/DFO}$+$BsAb_{\alpha\text{-EGFR}/\alpha\text{-PEG +/-FITC}}$ at varied ratios) were added to individual dishes in 250 µL volumes and incubated for the required times at 37°C with 5% CO_2. For all HBP incubated samples, 10 µg $HBP_{Cy5/DFO}$ was added per dish. BsAb and HBP_{Block} amounts were calculated based on specified stoichiometry to $HBP_{Cy5/DFO}$ at the specified timings. For pre-targeting samples, dishes were rinsed 3-fold with 1 mL PBS after removing BsAb containing media before adding either complete media, or complete media containing HBP as specified.

After the specified incubation times at 37°C with 5% CO_2, treatments were then removed and cells were washed twice with 1 mL PBS. Immediately, 200 µL of 4% PFA was added to cells for 10 minutes and washed three more times with 1 mL PBS.

Cells were imaged on a Leica SP8 scanning confocal microscope housed at the Australian Nanofabrication Facility Queensland Node. The Leica SP8 was equipped with a 40× water immersion lens and a white light laser (WLL). Images were collected using a sequential scanning method, with Cy5 and FITC being excited at 649 nm and 495 nm respectively. Corresponding fluorescence data was collected at 500-562 nm and 658-732 nm for FITC and Cy5 respectively.

1.5. *In vivo* imaging methods

1.5.1. ^{89}Zr radiolabelling

^{89}Zr preparation and conjugate radiolabelling followed our previously published methodology.[10] In brief, ^{89}Zr was received in 1 M oxalic acid and was neutralized with 75% (v/v) 1 M Na_2CO_3 before diluting with equal volume 0.5 M HEPES buffer (pH 7.5). Aliquots of neutralized ^{89}Zr stock were then added to DFO functionalized conjugates ($BsAb_{\alpha\text{-EGFR}/\alpha\text{-PEG/DFO}}$ or $HBP_{Cy5/DFO}$) to achieve desired excess of the conjugate to the radiometal (1000-fold for $HBP_{Cy5/DFO}$ or 500-fold for $BsAb_{\alpha\text{-EGFR}/\alpha\text{-PEG/DFO}}$). Samples were then incubated at 37 °C in a thermoshaker with agitation at 400 rpm for 1 hour. To confirm radiolabelling, 2 µL samples of each solution were taken and either spotted directly or incubated with 5 µL 50 mM diethylenetriaminepentaacetic acid (DTPA) for 5 minutes before being spotted on thin layer chromatography paper (Agilent iTLC-SG Glass microfiber chromatography paper impregnated with silica gel). TLC were then run with 50/50 (v/v) EtOH/H_2O as the eluent. Control experiments were conducted to monitor the elution behaviour of unbound ^{89}Zr or ^{89}Zr chelated by small molecule DFO species for quality control. Radioactivity in the TLC was then measured utilizing an Eckert and Zeigler Mini-Scan and Flow-Count (B-MS-1000F) radio-TLC detector. Radiolabelled constructs or free ^{89}Zr displayed an R_f of 0, while [^{89}Zr]DTPA or [^{89}Zr]DFO (small molecule chelator) showed an R_f of 1, allowing simple determination of both free ^{89}Zr or residual free chelator. All ^{89}Zr-labelled conjugates showed a radiopurity of ≥95% prior to injection.

1.5.2. Animal model

All studies were in accordance with guidelines of the Animal Ethics Committee of The University of Queensland (UQ; Approval AIBN/105/19), and Australian Code for the Care and

Use of Animals for Scientific Purposes. Female Balb/c nu/nu mice (approximately 8 weeks of age) were acquired from the Animal Resource Centre (Western Australia) and housed in temperature and humidity-controlled housing with *ad libitum* access to food and water.

MDA-MB-468 cells were cultured and harvested (above) before being resuspended at approximately 5 x 10^6 cells per 50 uL PBS and transported on ice to the animal house. Mice were anaesthetised using 2 % isofluorane in O_2 for all injection and imaging procedures throughout. Mice were injected (27 G needle, 50 µL PBS) with 5 x 10^6 MDA-MB-468 cells in the left mammary fat pad. Tumours were allowed to develop for 8 weeks before ^{89}Zr-labelled nanomedicine administration at which time they were approximately 100-150 mm^3 in volume.

1.5.3. Pre-targeting and ^{89}Zr-labelled material administration

Pre-targeting dosing regimens followed that outlined in the results section. For all pre-targeting injections of $BsAb_{\alpha\text{-EGFR}/\alpha\text{-PEG}}$ the injected mass was held at a constant 900 µg per animal in 200 µL PBS.

^{89}Zr-labelled constructs (Section S1.5.1) were taken and concentrated PBS added to achieve 1X PBS in the final prepared dose. All constructs were mass dosed as below to allow meaningful comparisons between dosing groups.

To determine pharmacokinetics of $BsAb_{\alpha\text{-EGFR}/\alpha\text{-PEG}}$ alone in pre-dosing injections, additional cold $BsAb_{\alpha\text{-EGFR}/\alpha\text{-PEG/DFO}}$ was added to [^{89}Zr]$BsAb_{\alpha\text{-EGFR}/\alpha\text{-PEG/DFO}}$ (Section S1.5.1) to achieve equivalent 900 µg administered BsAb per mouse while maintaining an imaging dose of 3.2-3.4 MBq injected activity per mouse.

In ^{89}Zr-labelled $HBP_{Cy5/DFO}$ doses, administered mass doses were maintained at 91 µg per mouse for all animals regardless of BsAb formulation. This resulted in an approximate 8-fold molar excess of BsAb injected per mouse in pre-targeted animals. Where [^{89}Zr]$HBP_{Cy5/DFO}$ was pre-mixed with BsAb prior to injection, PBS formulated [^{89}Zr]$HBP_{Cy5/DFO}$ was added to $BsAb_{\alpha\text{-EGFR}/\alpha\text{-PEG}}$ at a 1:1 BsAb:HBP ratio and allowed to stand at RT for 45 minutes prior to injection. All [^{89}Zr]$HBP_{Cy5/DFO}$ administered imaging doses were maintained at 2.5-3 MBq injected activity per mouse.

1.5.4. ^{89}Zr PET imaging

The authors acknowledge the facilities and scientific and technical assistance of the National Imaging Facility, a National Collaborative Research Infrastructure Strategy (NCRIS) capability, at the Centre for Advanced Imaging, The University of Queensland where this imaging work was undertaken.

PET-CT imaging followed our previously published methods.[10] In short, for dynamic biodistribution studies of [^{89}Zr]$BsAb_{\alpha\text{-EGFR}/\alpha\text{-PEG/DFO}}$, anaesthetized non-tumour bearing mice, with a cannulated tail vein, were positioned on the scanner bed and moved to the PET acquisition position. [^{89}Zr]$BsAb_{\alpha\text{-EGFR}/\alpha\text{-PEG/DFO}}$ was then injected (200 µL phosphate buffered saline) and dynamic images acquired over the first 60 minutes following injection. Subsequent static images were acquired at 5 and 21 hours post injection.

PET-CT images of nanomedicine behaviour were acquired at 8 hours, 22 hours, 2 days, 3 days and 6 days post [^{89}Zr]HBP$_{Cy5/DFO}$ administration.

All imaging utilized a Siemens Inveon PET-CT scanner with physiological monitoring achieved using a respiratory probe (BioVetTM system, m2m Imaging, Australia). Following each PET acquisitions (20-90 minutes), micro-CT scans were acquired for anatomical co-registration. The CT images of the mice were acquired through an X-ray source with the voltage set to 80 kV and the current set to 500 µA. The scans were performed using 360° rotation with 120 rotation steps with a low magnification and a binning factor of four. The exposure time was 240 ms with an effective pixel size of 102.34 µm. The total CT scanning process took approximately 15 minutes. The CT images were reconstructed using Feldkamp reconstruction software (Siemens).

The PET Images were reconstructed using an ordered-subset expectation maximization (OSEM2D) algorithm and analysed using the Inveon Research Workplace software (IRW 4.1) (Siemens) which allows fusion of CT and PET images and definition of regions of interest (ROIs). CT and PET datasets of each individual animal were aligned using IRW software (Siemens) to ensure good overlap of the organs of interest. Three dimensional ROIs were placed within the whole body, as well as all the organs of interest, such as heart, kidneys, bladder, liver, spleen, and tumour, using morphologic CT information to delineate organs. Lungs and bone ROIs were defined by threshold masking of images based on the differential CT density of these organs. Activity per voxel was converted to nci/cc using a conversion factor obtained by scanning a cylindrical phantom filled with a known activity of ^{89}Zr to account for PET scanner efficiency. Activity concentrations were then expressed as percent of the decay-corrected injected activity per cm^3 of tissue that can be approximate as percentage injected dose/g (%ID/g).

1.5.5. *Ex vivo* biodistribution

Following completion of final PET-CT images, animals were euthanised by cervical dislocation. Blood was sampled and tissues collected and cleaned of excess blood and weighed for ex vivo analysis. A PerkinElmer 2480 Automatic Gamma Counter was used to measure radioactivity in tissues. The gamma counter was calibrated using known samples of ^{89}Zr and measured activity presented as %ID/g based on injected activities.

2. Supplementary Information

2.1. Polymer synthesis and characterization

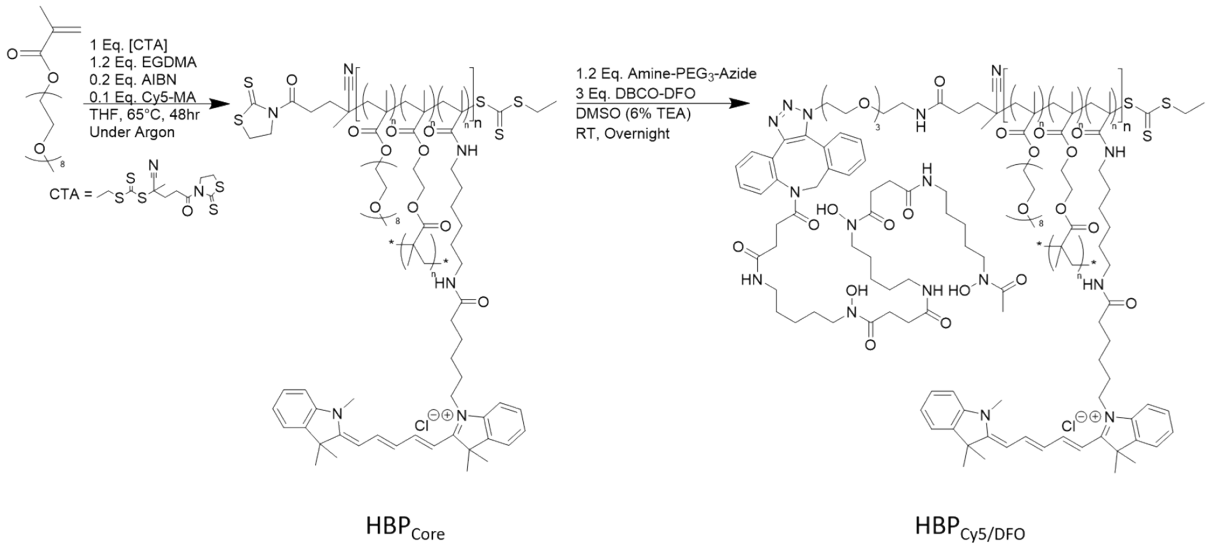

Figure S1. HBP synthesis steps to form first HBP_{Core} and then final $HBP_{Cy5/DFO}$ used for all biological assays

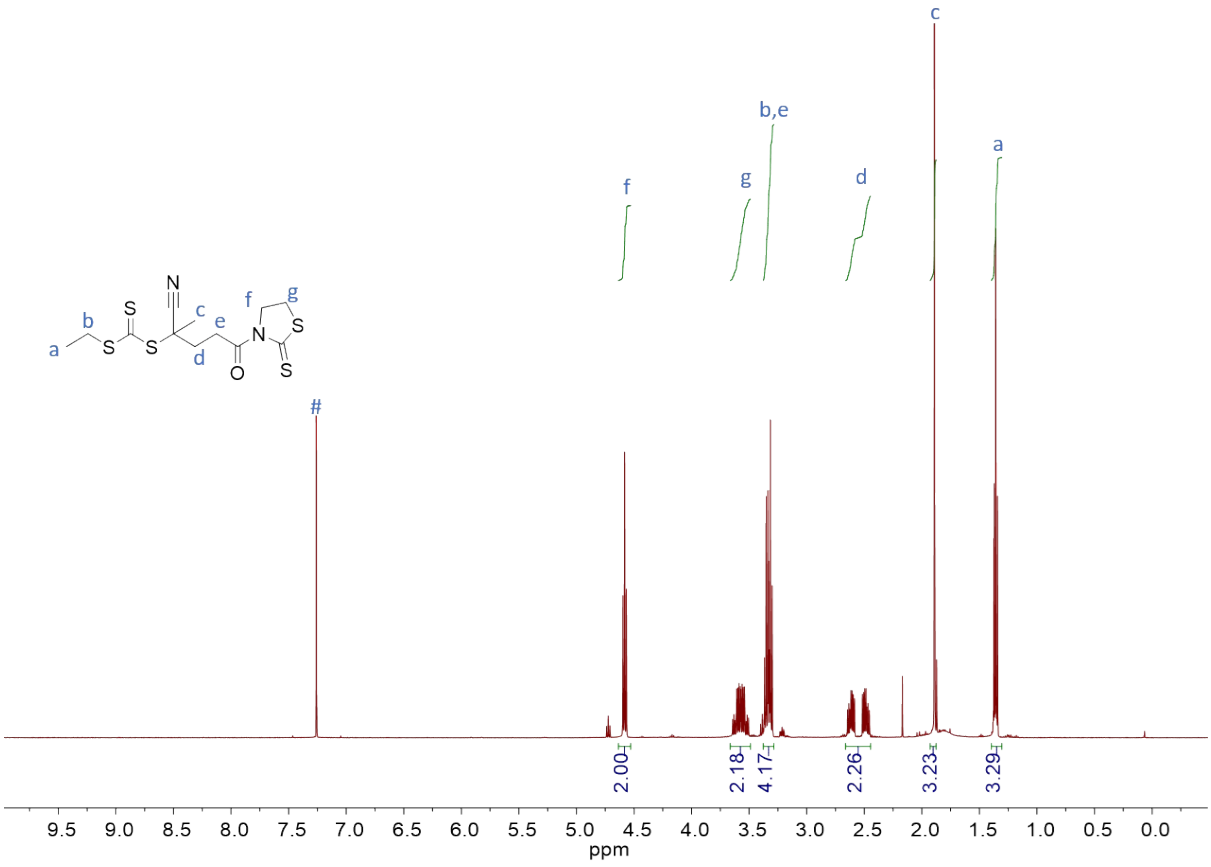

Figure S2. NMR spectra of synthesized CEPA-TT RAFT agent

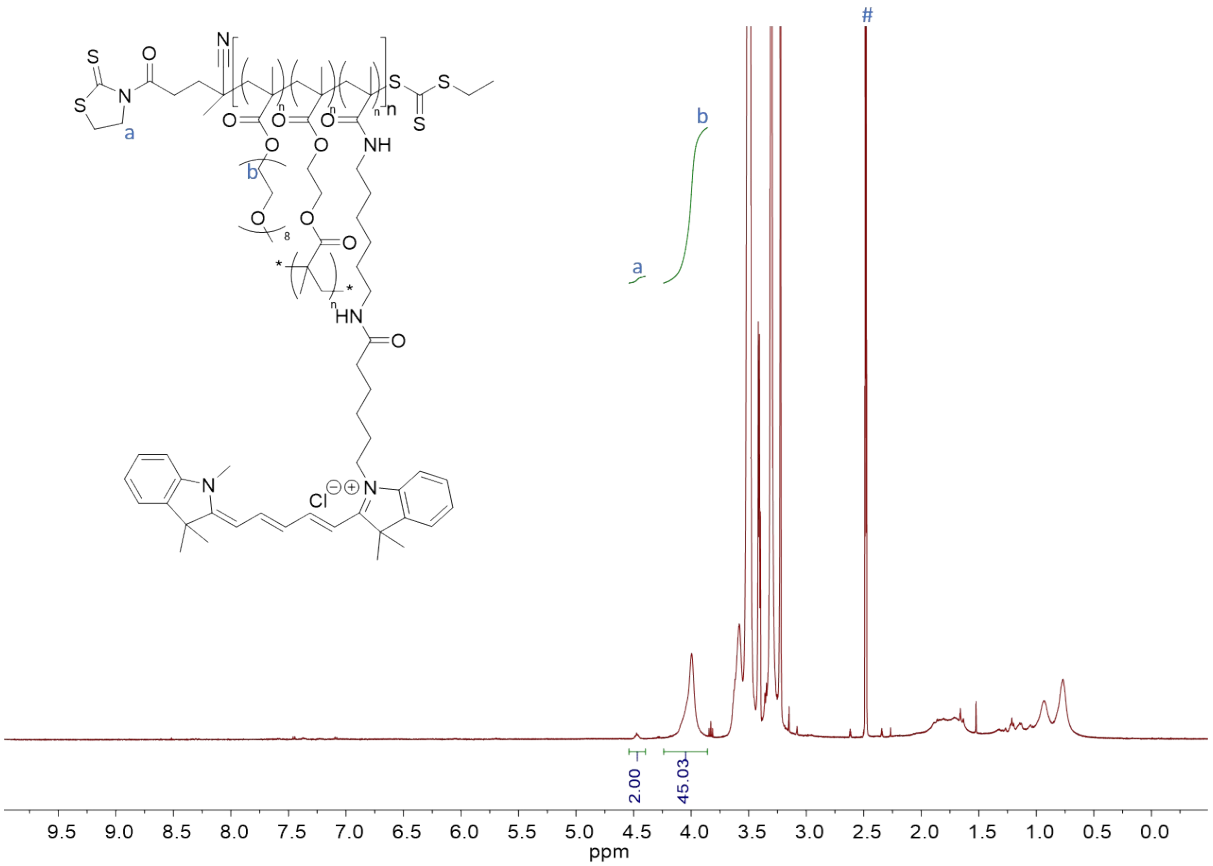

Figure S3. NMR spectra of HBP_{Core} incorporating thiazoline RAFT agent retained on chain ends

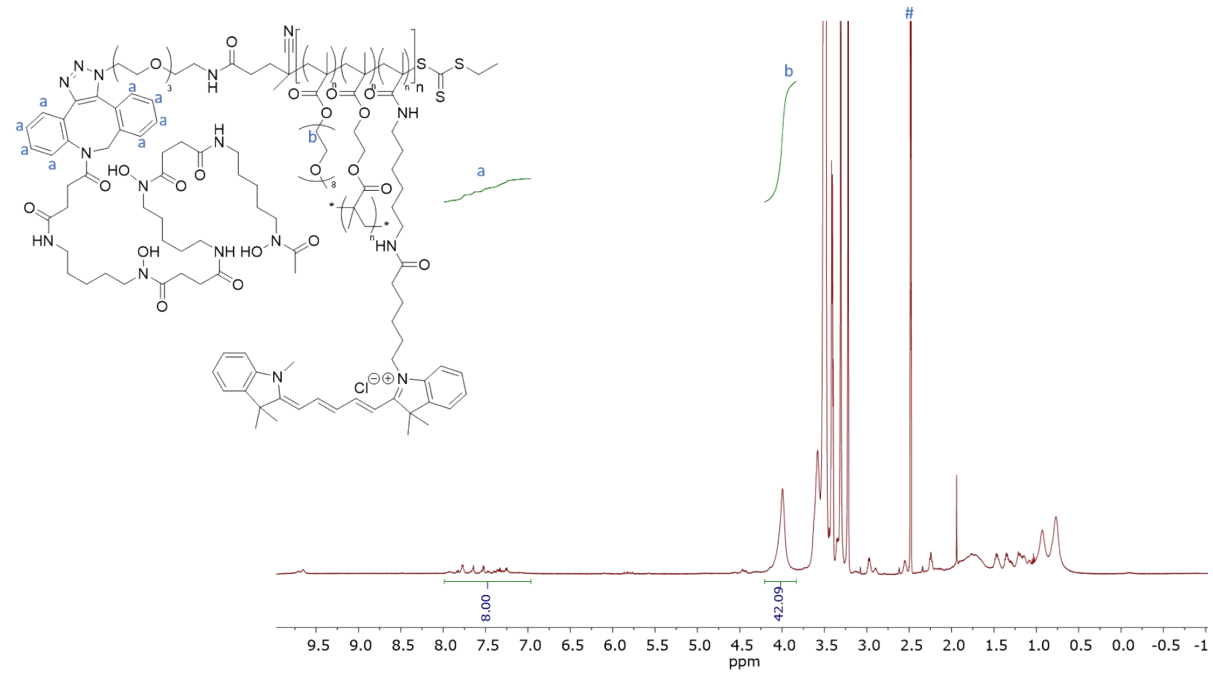

Figure S4. NMR spectra of $HBP_{Cy5/DFO}$ after sequential modification with Azido-PEG3-Amine followed by Deferoxamine-DFO attachment showing near quantitative functionalization of chain ends

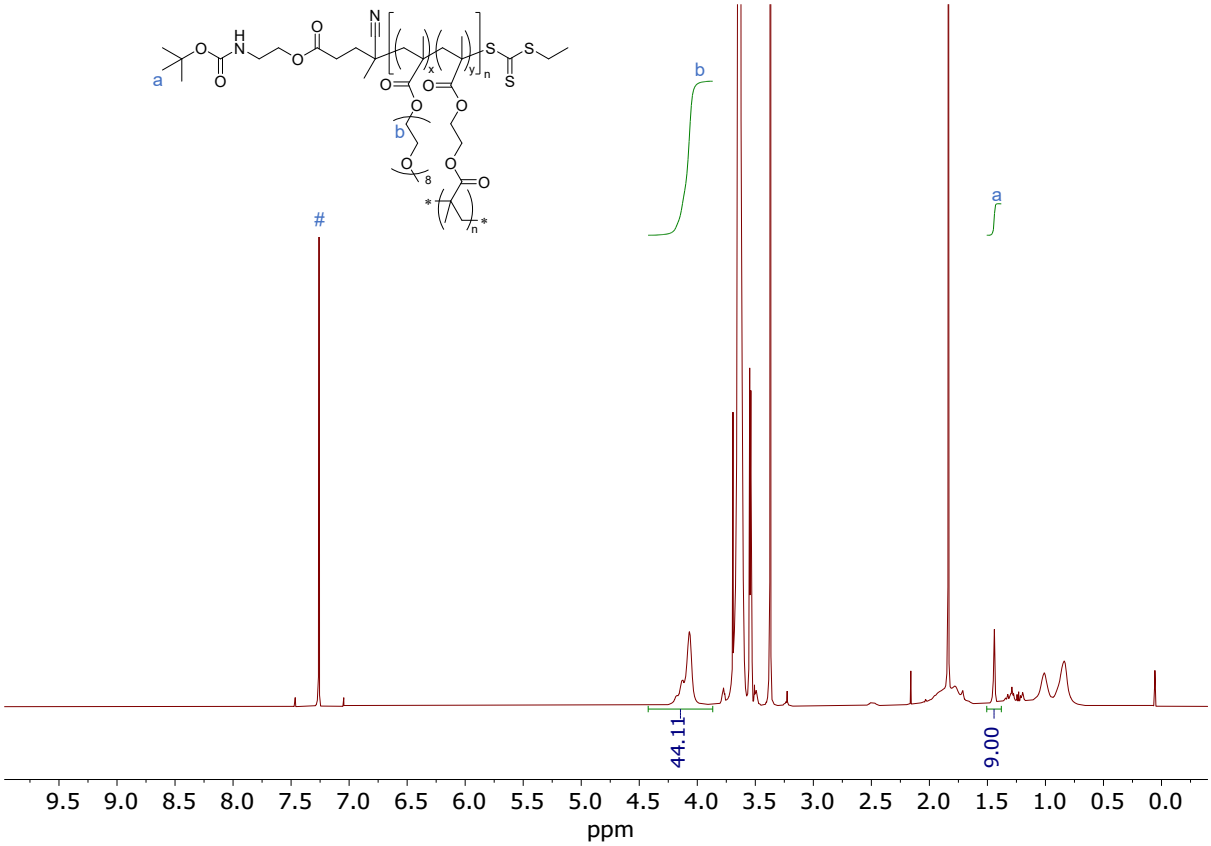

Figure S5. NMR spectra of HBP_{Block} incorporating BOC-amine CEPA RAFT agent retained on chain ends. # denotes residual solvent peak for $CHCl_3$

2.2. In vitro pre-targeting

2.2.1. Pre-targeting over 0-5 hours

Initial flow cytometry assays to validate cell-based pre-targeting followed methods in Section 1.4, with BsAb added at an 8:1 excess in pre-targeting samples, and all samples analysed after exposure to $HBP_{Cy5/DFO}$ formulations for 1 hour. Results are shown in Figure S6 and indicate that HBP alone shows minimal cellular association (<5% Cy5+), whereas the pre-targeting approach results in comparable association to that of HBP-BsAb premixing at a 1:3 ratio and there is minimal change when the pre-targeting timeframe is varied from 0-5 hours before HBP addition (all >93% Cy5+).

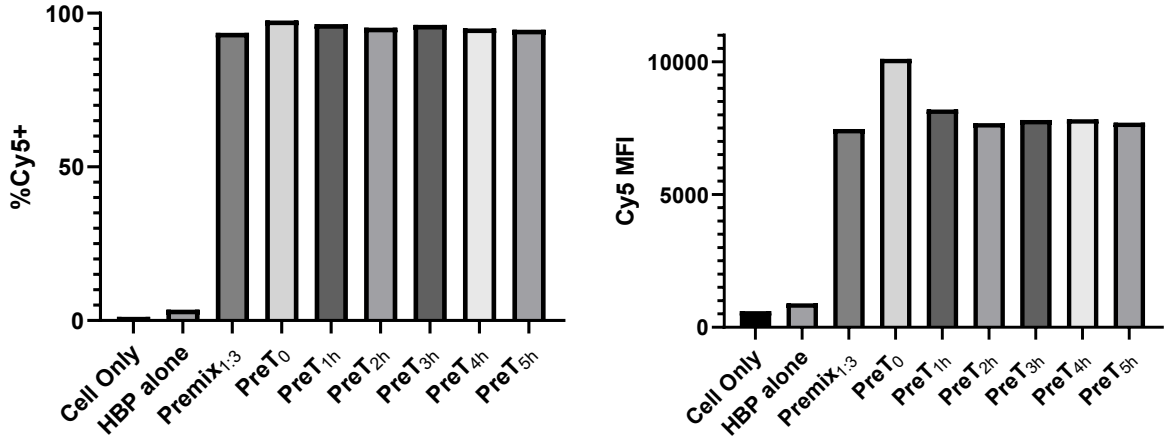

Figure S6. Flow cytometry validation of in vitro pre-targeting at 1 hour after HBP addition for 0-5 hours pre-targeting conditions

2.2.2. Pre-targeting after overnight incubations

Pre-targeting experiments were conducted to mirror those probed in Section 2.2.1 at extended timeframes to probe the longevity of pre-targeting strategy. In vitro pre-targeting assays followed methods in Section 1.4 and both flow cytometry and microscopy assays were carried out in parallel to allow comparison of results and probing of cellular localization of materials as well as association. Pre-targeting was assessed at 0 h, 4 h, 9 h or after overnight incubation (30 h) following removal of unbound $BsAb_{\alpha\text{-EGFR}/\alpha\text{-PEG/FITC}}$ before addition of HBP (1:10 HBP:BsAb initially added) and compared to premixed HBP-BsAb association. An additional premixed sample at 1:10 HBP:BsAb ratio to mirror the molar ratios used in pre-targeting strategies was also included as an additional control for stoichiometry. Microscopy and flow cytometry analysis was conducted at 1 hour after HBP addition.

Confocal microscopy of both $BsAb_{\alpha\text{-EGFR}/\alpha\text{-PEG/FITC}}$ and $HBP_{Cy5/DFO}$ components demonstrated that both were present primarily on the surface of the cells at 1 hour after HBP addition irrespective of pre-targeting incubation time, suggesting the BsAb alone is not readily internalized and remains on the cell surface where it is available to bind PEGylated materials.

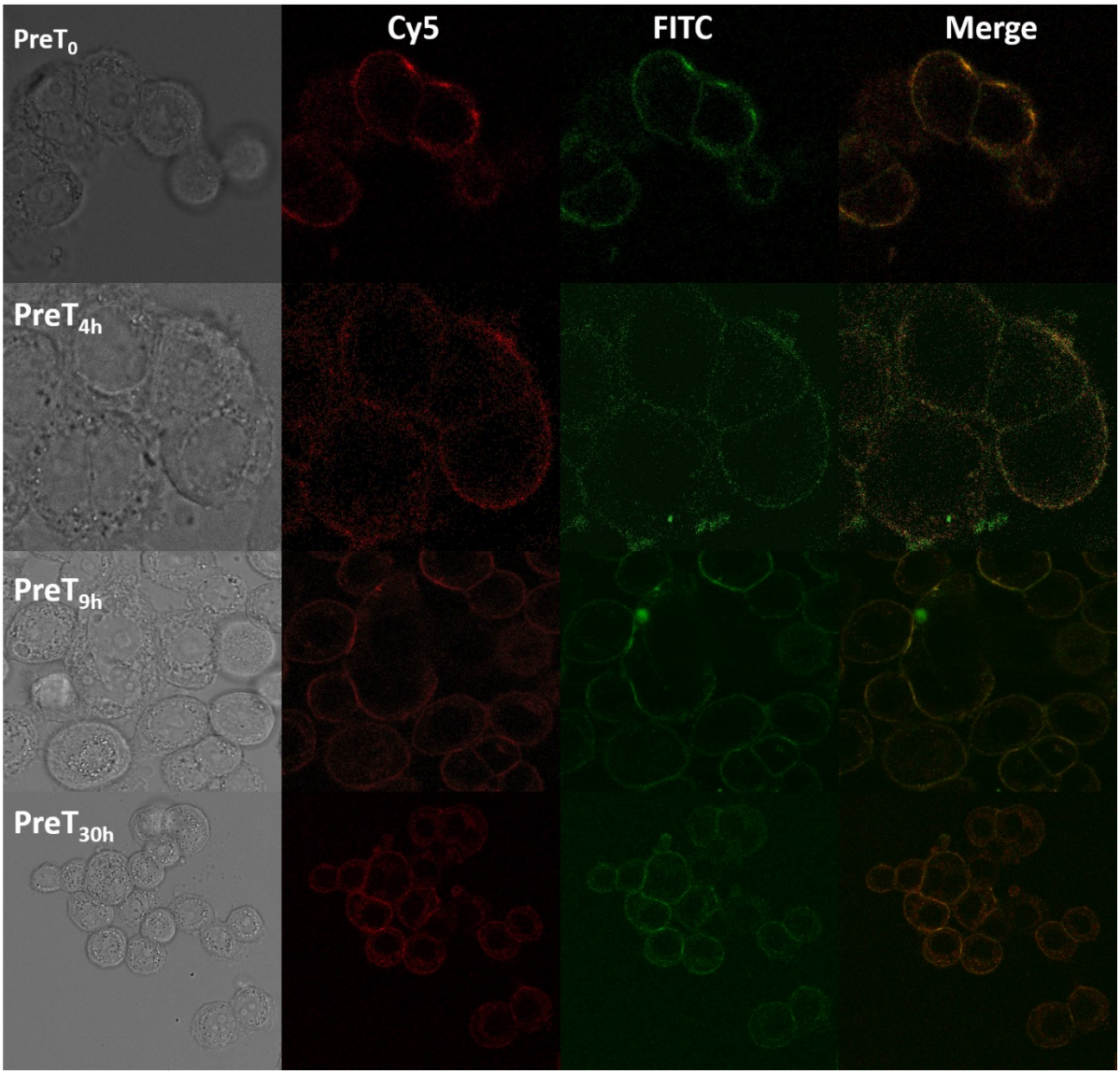

Figure S7. Microscopy images showing Cy5 ($HBP_{cy5/DFO}$) and FITC ($BsAb_{\alpha\text{-}EGFR/\alpha\text{-}PEG/FITC}$) signal 1 hour after addition of HBP at varied pre-targeting times after BsAb addition. All images were taken at 40x magnification.

Flow cytometry analysis of HBP association (Figure S8) showed that BsAb pre-targeting of HBP materials remained effective even after overnight incubation of pre-targeted cells. Results showed %Cy5+ of cells to remain at >88% even at 9 hours pre-targeting and reduced to 68% after extended overnight (30 hour) timeframes. This is commensurate with a gradual reduction in measured MFI until overnight pre-targeted samples Cy5 MFI were reduced to 28% of that measured when HBP was added immediately after excess BsAb was removed. The $Premix_{1:10}$ condition showed comparable cellular association to the $Premix_{1:3}$, however with marginal decrease in measured Cy5 MFI. This suggests that this high level of BsAb addition may be approaching the saturation of cellular receptors, however would require further study to probe this limit.

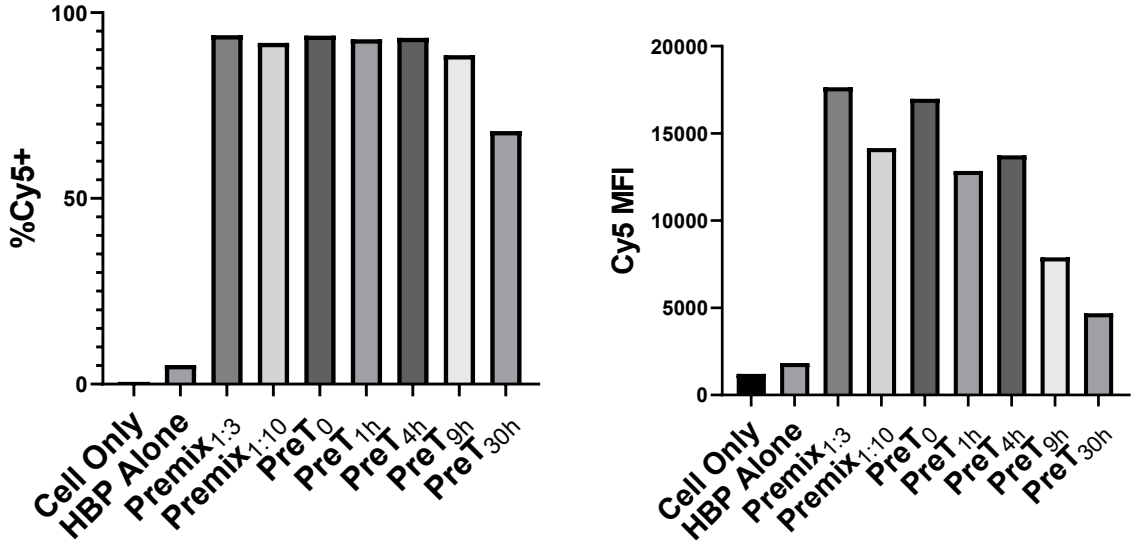

Figure S8. Flow Cytometry analysis of $HBP_{Cy5/DFO}$ cellular association following BsAb premixing or pre-targeting strategies

2.2.3. BsAb Cellular Association

Confocal microscopy of $BsAb_{\alpha\text{-EGFR}/\alpha\text{-PEG/FITC}}$ alone at the same timepoints as shown in Figure 2 and Figure Figure S7, showed comparable BsAb localization to that of $HBP_{Cy5/DFO}$ on MDA-MB-468 cells. These images in Figure S9 show the Bsab is primarily located on the cell surface for binding PEGylated materials at extended times.

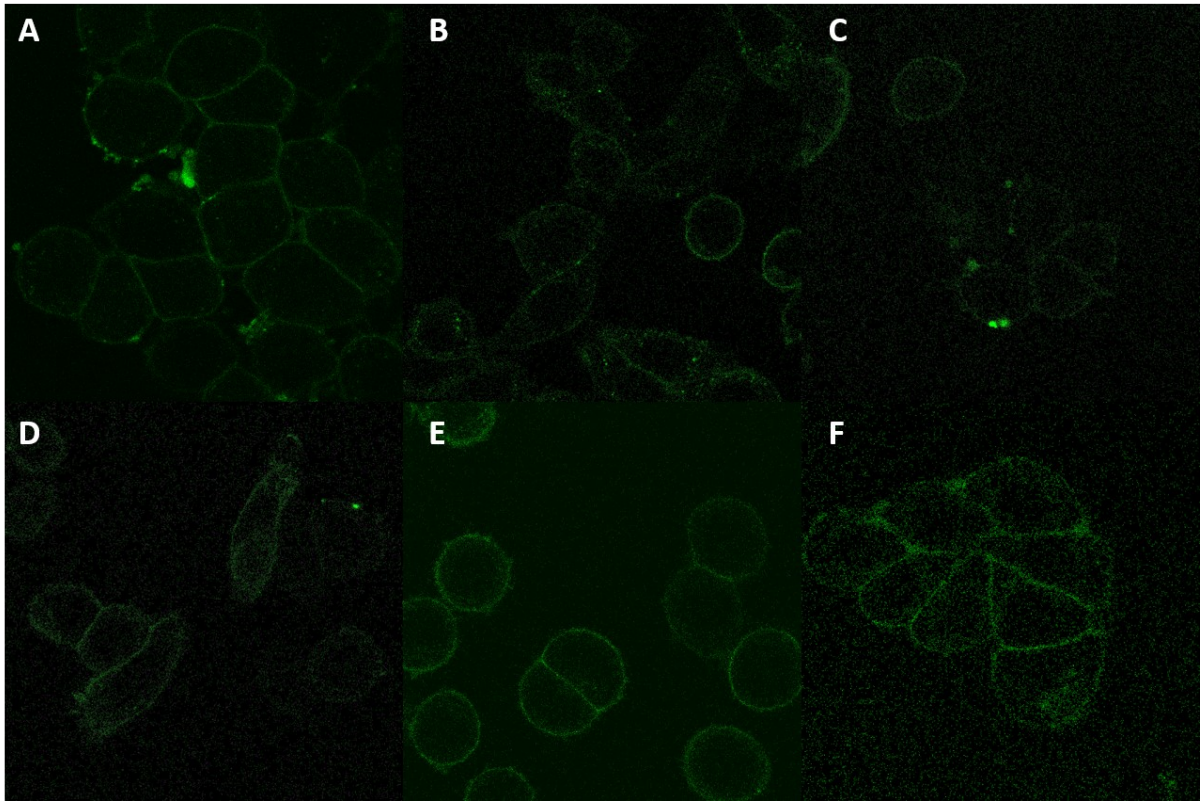

Figure S9 Microscopy images showing FITC signal of $BsAb_{\alpha\text{-EGFR}/\alpha\text{-PEG/FITC}}$ incubated alone with MDA-MB-468 cells over timepoints 0, 1, 2, 5, 10 and 31 hr shown in panels A-F respectively.

2.2.4. Cellular internalization

Confocal microscopy was utilized to assess cellular internalization of HBP materials after either premixing or pre-targeting strategies in comparison to HBP added alone. Equivalent masses of $HBP_{CY5/DFO}$ was added either alone, after premixing with a 3:1 excess of BsAb or 1 hour after removal of unbound BsAb (initially added at 10:1 excess) from MDA-MB-468 cells. Microscopy (Figure S10A) shows minimal uptake of HBP alone as expected for low fouling PEG-based materials. In comparison both premixed (Figure S10B) and pre-targeted (Figure S10C) approaches generated significant levels of HBP internalization, with observable HBP signal primarily imaged in punctate regions within the cells, likely a result of receptor mediated internalization.

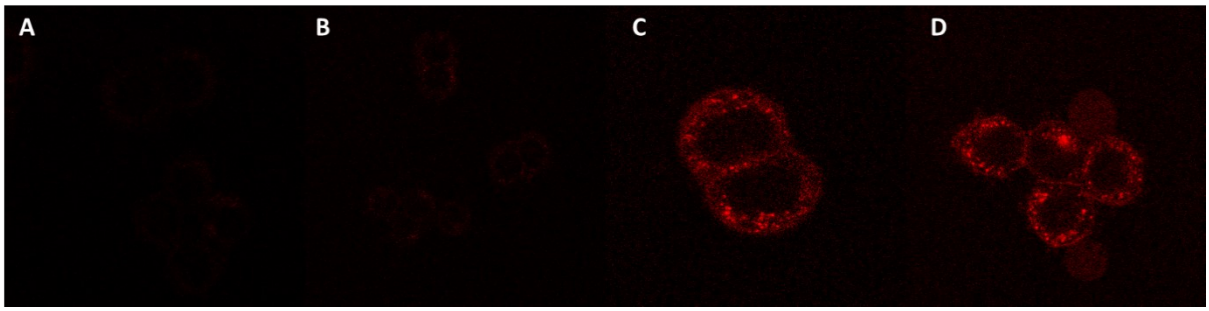

Figure S10. Microscopy images showing Cy5 ($HBP_{cy5/DFO}$) signal for HBP alone at 1 Hr A) and 4 Hr B) timepoints, C) premixed HBP/BsAb and D) $PreT_1$ were both imaged at 4 hours after HBP addition. All images were taken at 40x magnification.

2.2.5. Pre-targeting blocking

To validate the pre-targeting strategy driving cellular association and uptake through recognition of mPEG epitopes by surface bound $BsAb_{\alpha\text{-EGFR}/\alpha\text{-PEG}}$, cellular association studies were repeated with the addition of 2 to 200-fold excess of HBP_{Block}, a non-dye labelled PEG based HBP control material in an effort to saturate available BsAb binding sites.

Flow cytometry results (Figure S11) showed effective blockade of $BsAb_{\alpha\text{-EGFR}/\alpha\text{-PEG}}$ mediated $HBP_{Cy5/DFO}$ uptake. A 20-fold excess of HBP_{Block} largely inhibited cellular association of $HBP_{Cy5/DFO}$, with MFI reduced to only 15% of the unblocked $PreT_0$ sample. At 200-fold excess of $HBP_{Block,}$ MFI was further reduced to only 31% higher than background non-specific HBP uptake in the absence of targeting BsAb.

To further probe the stoichiometry required to mediate cellular association in the pre-mixed targeting strategy A comparison of $Premix_{1:1}$ and $Premix_{1:3}$ HBP:BsAb was also undertaken (Figure S11). Flow cytometry results demonstrate minimal difference in the resulting cellular association, suggesting that a 1:1 ratio of targeting BsAb to HBP in the premixed targeting approach is likely sufficient to facilitate cellular targeting while minimizing immunogenic clearance of injected materials.

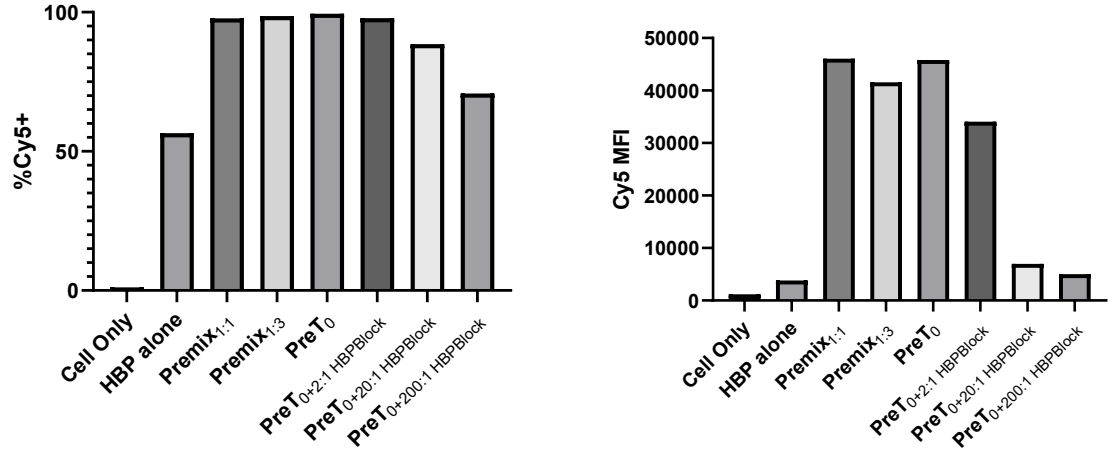

Figure S11. Flow cytometry analysis of pre-targeting uptake of HBP by BsAb specificity through addition of excess blocking HBP

2.3. In Vivo pre-targeting

2.3.1. $[^{89}Zr]BsAb_{\alpha\text{-EGFR}/\alpha\text{-PEG}}$ pharmacokinetics and biodistribution

BsAb was functionalized with the ^{89}Zr chelator DFO to give $BsAb_{\alpha\text{-EGFR}/\alpha\text{-PEG/DFO}}$. Chelator functionalized BsAb was then radiolabelled with ^{89}Zr (Section 1.5.1) to give $[^{89}Zr]BsAb_{\alpha\text{-EGFR}/\alpha\text{-PEG/DFO}}$ which was then administered to naïve female balb/c nude mice and imaged over the 1st hour following administration and subsequently at 5 and 21 hours post injection. ROI analysis of tissues allowed quantitative determination of BsAb biodistribution (Figure S12) and was further validated through ex vivo gamma-counter analysis of tissues following the terminal 21 hour image (Figure S13). BsAb was cleared rapidly from circulation, primarily through hepatic pathways. Splenic accumulation was also elevated at later timepoints, congruent with expected clearance of exogenous proteins from circulation, likely by the

mononuclear phagocytic system. BsAb was also noted to be retained in the kidneys, even at 21 hours post administration. This is likely a result of catabolism of administered BsAb DFO conjugates, the resulting radio-labelled fragments of which are absorbed during renal filtration but do not readily undergo trafficking and are retained in the tissues.[11]

The heart ROI was utilized as a measure of circulating radiolabelled material on the assumption of no specific interaction with cardiac tissue. This was then fit to a two-phase exponential decay (Figure S14) which models initial (fast) distribution throughout the body followed by an elimination (slow) phase. Fitting showed an elimination half-life of 17.5 minutes following administration of 900 µg BsAb which is equivalent to the dose used throughout subsequent pre-targeting imaging experiments.

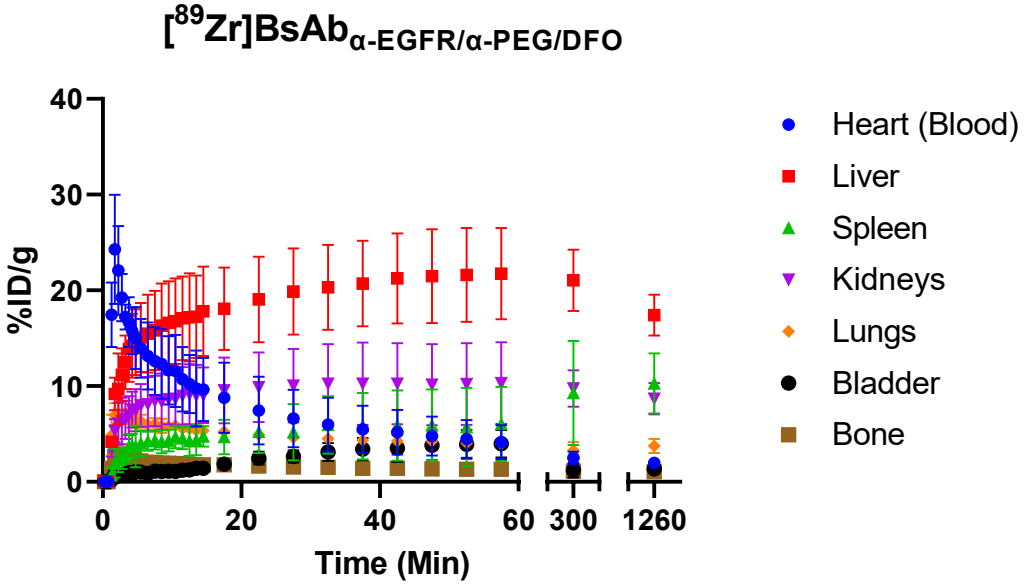

Figure S12. ROI analysis of ^{89}Zr-PET imaging following administration of [^{89}Zr]BsAb$_{\alpha\text{-EGFR}/\alpha\text{-PEG}/\text{DFO}}$ to naïve balb/c mice

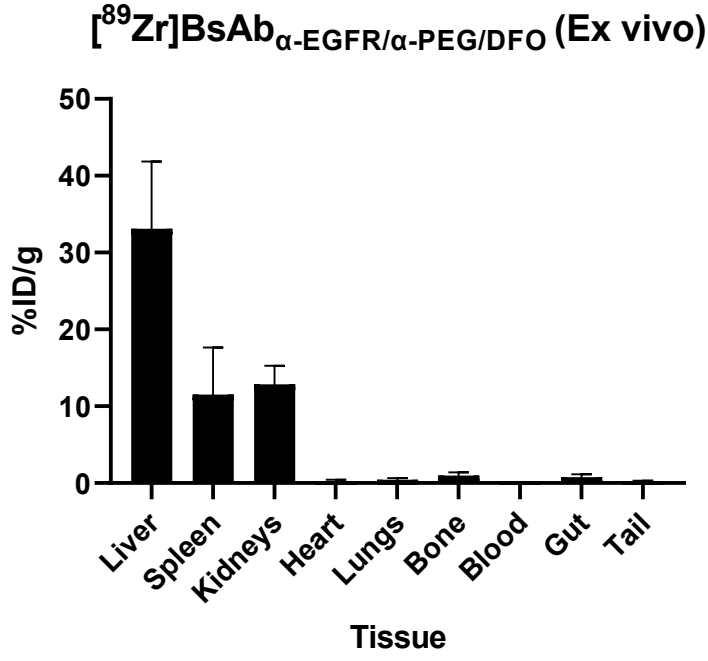

Figure S13. Ex vivo γ counter analysis of [^{89}Zr]BsAb$_{\alpha\text{-EGFR}/\alpha\text{-PEG/DFO}}$ biodistribution at 21 hours after administration

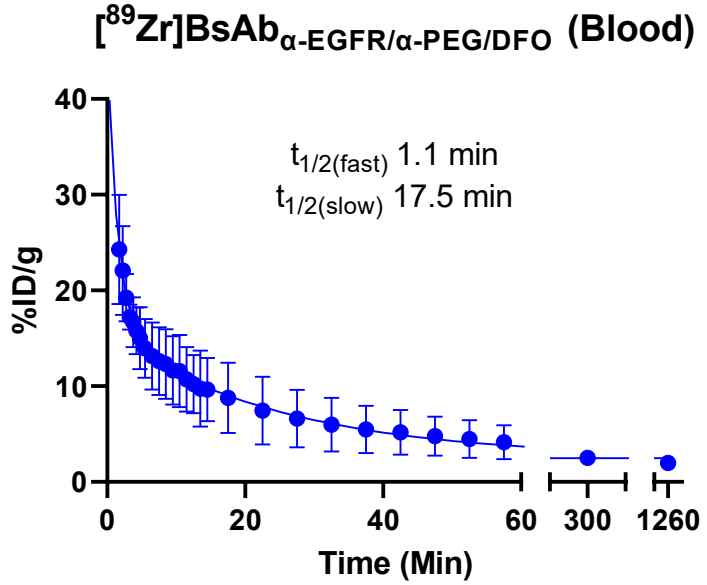

Figure S14. Two-phase exponential fit of circulating levels of [^{89}Zr]BsAb$_{\alpha\text{-EGFR}/\alpha\text{-PEG/DFO}}$ following injection

2.3.2. [^{89}Zr]HBP$_{Cy5/DFO}$ pre-targeting in vivo

Pre-targeting of HBP$_{Cy5/DFO}$ was then explored in a preclinical MDA-MB-468 orthotopic breast cancer model. HBP$_{Cy5/DFO}$ was radiolabelled as described in Section 1.5.1 and administered as described in Section 1.5.3. The BsAb$_{\alpha\text{-EGFR}/\alpha\text{-PEG}}$ pre-dosing was conducted at consistent mass dosing and designed to match the mass dosing used in the imaging study of [^{89}Zr]BsAb$_{\alpha\text{-EGFR}/\alpha\text{-PEG}/DFO}$ alone (Section 2.3.1) to control for any changes in pharmacokinetics resulting from changes in administered dose. Similarly, [^{89}Zr]HBP$_{Cy5/DFO}$ was administered at consistent mass doses for all animals regardless of formulation to allow for direct comparison of resulting biodistribution.

Animals were dosed as described and then imaged at 8 hours, 22 hours, 2 days, 3 days and 6 days post [^{89}Zr]HBP$_{Cy5/DFO}$ administration. ROI analysis of tissues of interest allowed quantitation of HBP biodistribution in response to the targeting strategy employed (Figure S15A-E) and was further validated by ex vivo gamma counting of collected tissues after the terminal 6 day imaging timepoint (Figure S15F). Ex vivo analysis showed comparable trends for all measured in vivo data. Notably, the spleen is commonly difficult to measure accurately from in vivo data and in many cases presents an underestimate of true accumulation per gram of tissue which is best assessed by ex vivo quantitation as observed here, however overall trends remained consistent between analysis methods.

Figure S16 shows circulating (as measured by ROI of the heart) levels of [^{89}Zr]HBP$_{Cy5/DFO}$ for each targeting strategy compared to HBP alone. PreT$_{1h}$ shows the lowest circulating level followed by PreT$_4$h and premixed approaches with PreT$_{9h}$ showing circulation comparable to HBP alone.

Figure S17 shows tumour:liver ratios for each premixed and pre-targeted strategy compared to HBP alone. Premixed, PreT$_{1h}$ and PreT$_{4h}$ all show significantly reduced tumour:liver ratios compared to HBP, suggesting enhanced hepatic clearance of these targeting approaches. Comparatively, PreT$_{9h}$ shows enhanced (almost 2-fold) tumour:liver ratios compared to HBP alone.

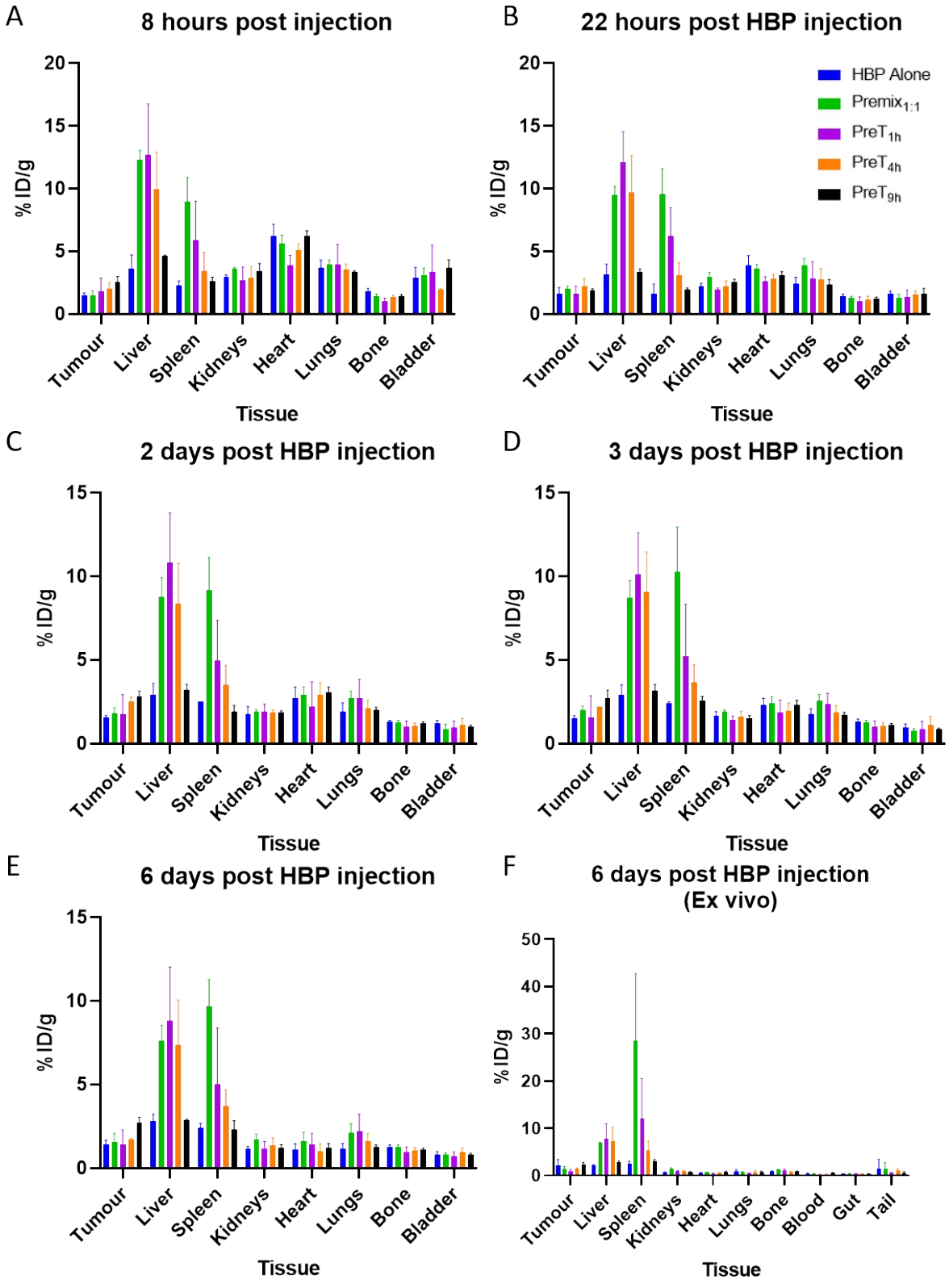

Figure S15. [^{89}Zr]HBP$_{Cy5/DFO}$ biodistribution in orthotopic preclinical breast cancer model following various targeting and formulation approaches. A-E) ROI analysis of [^{89}Zr]PET images for in vivo biodistribution at 8 hours to 6 days post injection, F) Ex vivo gamma counting analysis of the same animals to validate in vivo results.

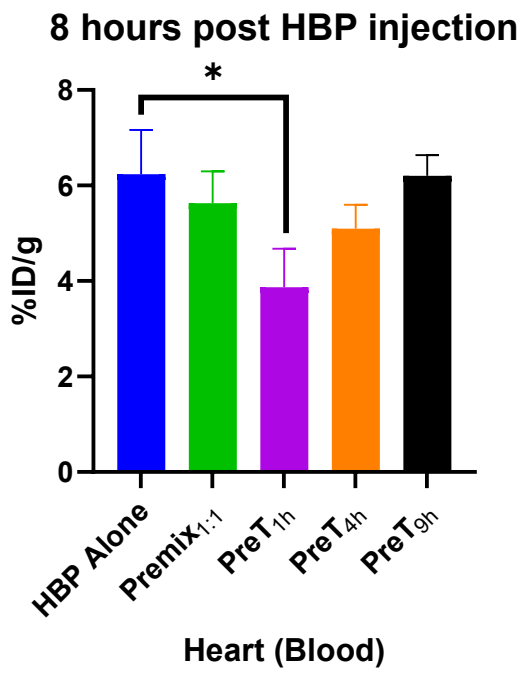

Figure S16. Heart (Blood) levels of [^{89}Zr]HBP$_{Cy5/DFO}$ at 8 hours post administration for each dosing formulation

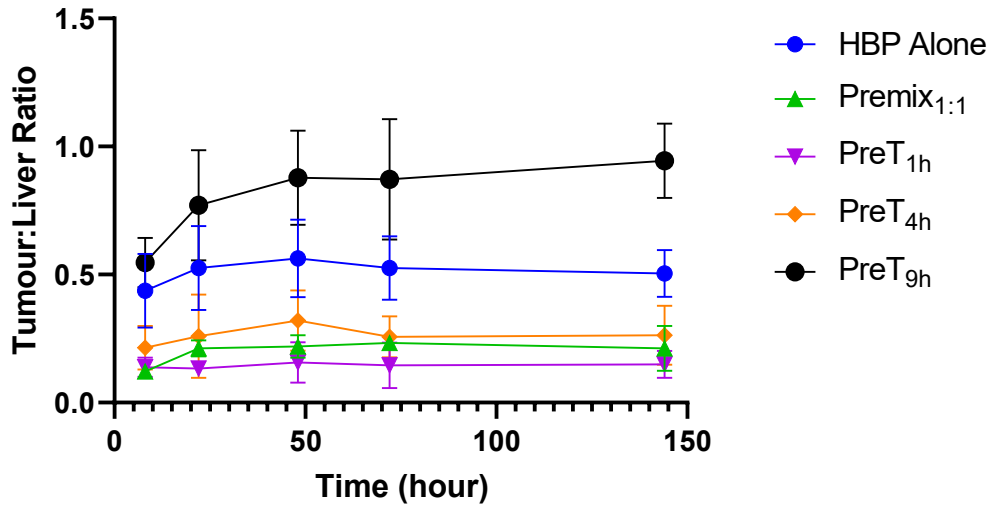

Figure S17. Tumour:Liver ratio for Premixed and Pre-targeting strategies compared to HBP alone over time

2.3.3. Blocking of [^{89}Zr]HBP$_{Cy5/DFO}$ pre-targeting in vivo

A blocking study was undertaken following the PreT$_{4h}$ dosing regimen with the addition of 200-fold excess of HBP$_{Block}$ at the time of administration of [^{89}Zr]HBP$_{Cy5/DFO}$. Figure S18 shows the resulting biodistribution of PreT$_{4h+Blocking}$ from 8 hours to 6 days post administration in comparison to HBP alone and PreT$_{4h}$. This shows that at all timepoint, biodistribution of [^{89}Zr]HBP$_{Cy5/DFO}$ is returned to close to that of HBP alone in the PreT$_{4h+Blocking}$ dosing regimen.

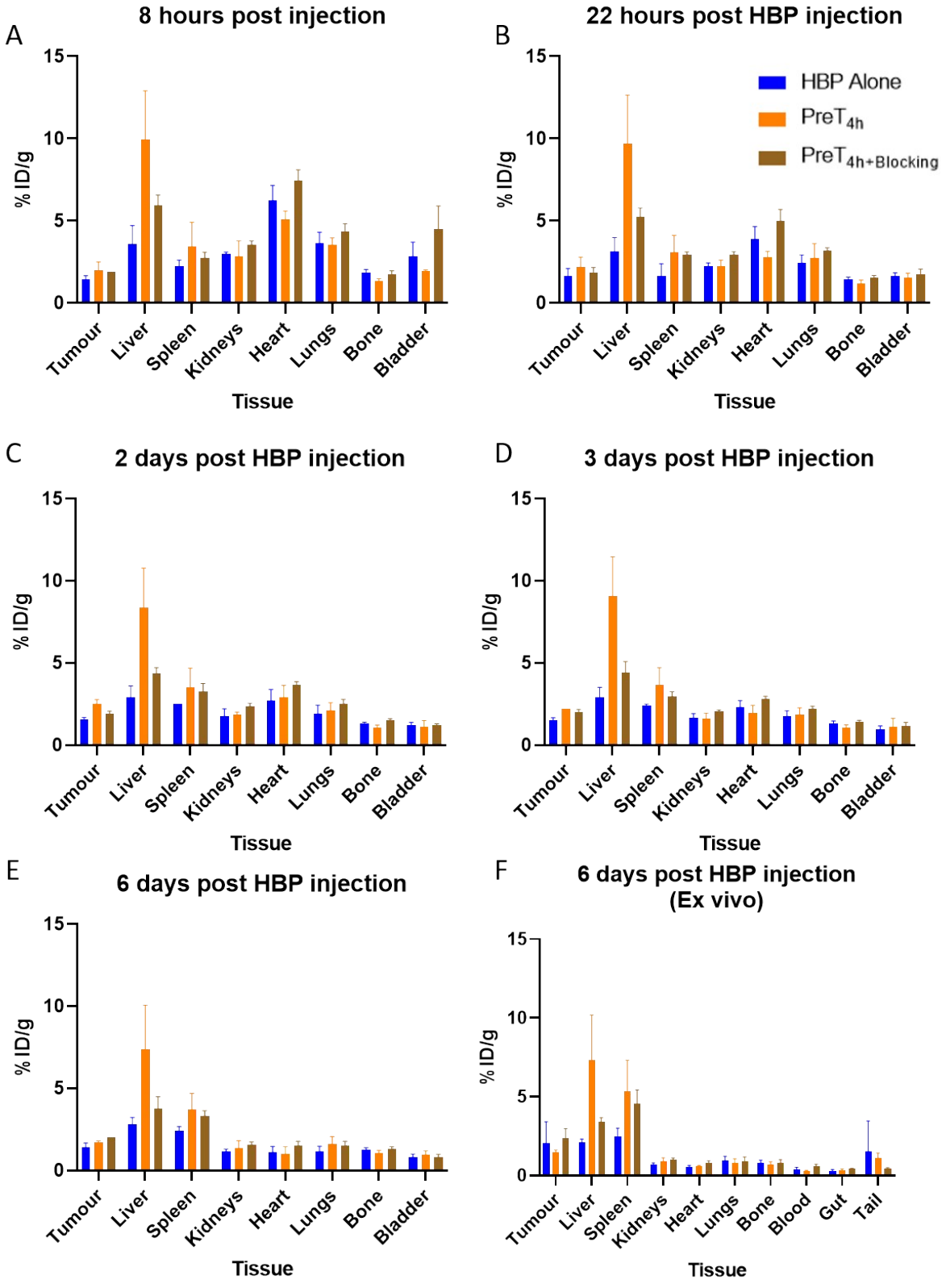

Figure S18. [^{89}Zr]HBP$_{Cy5/DFO}$ biodistribution in orthotopic preclinical breast cancer model comparing PreT$_{4h}$ approach with and without HBP blocking to HBP alone. A-E) ROI analysis of [^{89}Zr]PET images for in vivo biodistribution at 8 hours to 6 days post injection, F) Ex vivo gamma counting analysis of the same animals to validate in vivo results

References

1. A. J. Convertine, D. S. W. Benoit, C. L. Duvall, A. S. Hoffman and P. S. Stayton, *Journal of Controlled Release*, 2009, **133**, 221-229.
2. G. R. Ediriweera, J. D. Simpson, A. V. Fuchs, T. K. Venkatachalam, M. Van De Walle, C. B. Howard, S. M. Mahler, J. P. Blinco, N. L. Fletcher, Z. H. Houston, C. A. Bell and K. J. Thurecht, *Chemical Science*, 2020, **11**, 3268-3280.
3. E. T. Nadres, H. Takahashi and K. Kuroda, *Journal of Polymer Science Part A: Polymer Chemistry*, 2017, **55**, 304-312.
4. C. B. Howard, N. Fletcher, Z. H. Houston, A. V. Fuchs, N. R. Boase, J. D. Simpson, L. J. Raftery, T. Ruder, M. L. Jones, C. J. de Bakker, S. M. Mahler and K. J. Thurecht, *Adv Healthc Mater*, 2016, **5**, 2055-2068.
5. A. K. Pearce, J. D. Simpson, N. L. Fletcher, Z. H. Houston, A. V. Fuchs, P. J. Russell, A. K. Whittaker and K. J. Thurecht, *Biomaterials*, 2017, **141**, 330-339.
6. C. B. Howard, N. Fletcher, Z. H. Houston, A. V. Fuchs, N. R. B. Boase, J. D. Simpson, L. J. Raftery, T. Ruder, M. L. Jones, C. J. de Bakker, S. M. Mahler and K. J. Thurecht, *Advanced Healthcare Materials*, 2016, **5**, 2055-2068.
7. J. Cui, R. De Rose, K. Alt, S. Alcantara, B. M. Paterson, K. Liang, M. Hu, J. J. Richardson, Y. Yan, C. M. Jeffery, R. I. Price, K. Peter, C. E. Hagemeyer, P. S. Donnelly, S. J. Kent and F. Caruso, *ACS Nano*, 2015, **9**, 1571-1580.
8. Z. H. Houston, J. Bunt, K.-S. Chen, S. Puttick, C. B. Howard, N. L. Fletcher, A. V. Fuchs, J. Cui, Y. Ju, G. Cowin, X. Song, A. W. Boyd, S. M. Mahler, L. J. Richards, F. Caruso and K. J. Thurecht, *ACS Central Science*, 2020, **6**, 727-738.
9. P. W. Janowicz, Z. H. Houston, J. Bunt, N. L. Fletcher, C. A. Bell, G. Cowin, C. B. Howard, D. Taslima, N. Westra van Holthe, A. Prior, V. Soh, S. Ghosh, J. Humphries, P. Huda, S. M. Mahler, L. J. Richards and K. J. Thurecht, *Biomaterials*, 2022, **283**, 121416.
10. N. L. Fletcher, Z. H. Houston, J. D. Simpson, R. N. Veedu and K. J. Thurecht, *Chemical Communications*, 2018, **54**, 11538-11541.
11. C. T. Mendler, T. Gehring, H. J. Wester, M. Schwaiger and A. Skerra, *J Nucl Med*, 2015, **56**, 1112-1118.